Preparation, Characterisation, and Intramolecular Electron-transfer Studies on the Penta-ammineruthenium Histidine-modified High-potential Iron–Sulphur Protein from *Chromatium vinosum*†

Martin P. Jackman, Meng-Chay Lim, and A. Geoffrey Sykes *
Department of Chemistry, The University, Newcastle upon Tyne NE1 7RU
G. Arthur Salmon
Cookridge Radiation Research Centre, Leeds LS16 6QB

The high-potential iron–sulphur protein (Hipip) from *Chromatium vinosum* (M_r *ca.* 9 500; 85 amino acids) contains a single histidine residue, His 42, the location of which is known from the *X*-ray crystal structure. The reaction of $Hipip_{red}$ with excess $[Ru(NH_3)_5(H_2O)]^{2+}$ followed by oxidation, yields the Ru-modified protein $Hipip_{ox}$·Ru^{III}. The product has been purified by column chromatography, and analysed by inductively coupled plasma atomic emission spectroscopy (Fe:Ru ratio 4:1). The His 42 of the Ru-modified protein no longer reacts with diethyl pyrocarbonate (depc), and the sharp ^1H n.m.r. C_2H resonance of His 42 at 8.3 p.p.m. is no longer present due to paramagnetic line broadening by the attached Ru^{III}. The reduction potential of the $[Fe_4S_4]^{3+/2+}$ couple remains at 350 mV in the Ru^{III}-modified protein. On pulse radiolysis using e_{aq}^- ($CO_2^{\bullet -}$ or O_2^-) as reductant to generate $Hipip_{ox}$·Ru^{II}, a second stage assigned to intramolecular formation of $Hipip_{red}$·Ru^{III} is observed, $k = 18\ s^{-1}$ (pH 7.0, 20 °C). An additional step is observed as a result of autoreduction of $Hipip_{ox}$·Ru^{III} to $Hipip_{red}$·Ru^{III}, which occurs on bubbling Ar gas through solutions in anaerobic procedures. Subsequent pulsing generates some $Hipip_{red}$·Ru^{II}, the decay of which gives rise to a third stage here assigned as an intermolecular electron transfer between fully oxidised and fully reduced Ru-modified protein. The His 42 is near to the Fe_4S_4 active site, with Cys 43 attached to one of the Fe atoms. The direct donor–acceptor linkage is unusually short and the intramolecular rate constant is therefore of interest in the context of through-space (7.9 Å) or through-bond (13 Å) electron transfer. There is no obvious enhancement of the intramolecular electron-transfer process, and at this time no reason for favouring the through-bond assignment.

High-potential iron–sulphur protein (Hipip) from *Chromatium vinosum* is an acidic protein, p*I* = 3.88 (oxidised form) and 3.68 (reduced).[1] The estimated charge is −3 for the oxidised protein at pH ~ 7.0 from the amino-acid sequence[2] [one histidine (His) and two arginine (Arg) residues are assumed to be positively charged]. It consists of a single polypeptide chain of 85 amino acids,[2] and a [4Fe–4S] active site. Comparisons with six other complete Hipip sequences[3] reveal just seven invariant residues, including four cysteines (SR), which are attached to the core to give $Fe_4S_4(SR_4)$. The other invariant residues are Tyr 19, Asn 45, and Gly 75, all in close proximity to the active site. Three of the seven sequences are closely related (~70% conservation), but the others give much greater divergence than is observed with, for example, cytochrome c and plastocyanin.[4,5] Conservation of charge between the different Hipip sequences is also poor. However, the single surface histidine at position 42 in the *C. vinosum* sequence is conserved in four of the seven Hipip molecules thus far sequenced, and appears nearby at position 44 in a fifth (*T. pfennigii*).

X-Ray crystal structure information is available for both oxidation states of *C. vinosum*,[6,7] here designated $Hipip_{ox}$ and $Hipip_{red}$. The structural similarity of the cuboidal [4Fe–4S] core of Hipip, and of the 2[4Fe–4S] centres in ferredoxins (Fd) such as that from *Peptococcus aerogenes*,[8] is to be noted. Different redox changes are involved however, with reduction potentials of *ca.* −400 mV for Fd and +350 mV for *C. vinosum* Hipip,[1] which has led to the three-state hypothesis of Carter *et al.*[9,10] More recently the Fd and Hipip Fe_4S_4 active sites have been modelled.[11,12] Oxidation state levels $[Fe_4S_4]^{3+/2+}$ for Hipip, and $[Fe_4S_4]^{2+/+}$ for Fd, are supported by extensive spectroscopic evidence, including e.s.r., n.m.r., and Mössbauer studies,[13–16] which are consistent with isoelectronic and essentially diamagnetic ground states for $Hipip_{red}$ and Fd_{ox}. Different core, Fe–S bond distances have been identified for the different states.[7] The tertiary structure of Hipip can be viewed as two distinct domains, one binding the Fe_4S_4 core in a hydrophobic pocket and the second in effect burying the remaining exposed edge of the Fe_4S_4 unit. The His 42 residue is positioned at the interface of these sections with its side-chain protruding into solution.[6] The $[Fe_4S_4(SR)_4]^-$ cluster, the S atoms of which are at least 3.5 Å from the surface, is in contact with a large number of hydrophobic and other non-polar groups in the 'binding-pocket.' There are also several NH···S hydrogen bonds between the cysteinyl sulphur or core sulphides and the peptide backbone. Within the limits of the crystal structure information the only conformational changes detected in the peptide chain as a result of one-electron reduction are the small contractions in the NH···S contacts. It has been suggested that the extent of delocalisation of negative charge by NH···S interactions may be an important factor in the control of the Fe_4S_4 redox change.[10] There are also some changes in the core dimensions.

Recently the properties of 13 Hipip molecules have been compared.[17] The solution reactivity of *C. vinosum* Hipip has been extensively explored.[18–22]

Experimental

Protein Modification.—Extraction and purification of *C. vinosum* Hipip was carried out as previously described.[1,18] The

† *Non-S.I. unit employed:* M = mol dm^{-3}.

strain of *C. vinosum* used in these studies was NC1B 10441. Frozen cells were obtained from the PHLS Centre, Porton, U.K. The oxidised ($Hipip_{ox}$) and reduced ($Hipip_{red}$) forms, $[Fe_4S_4]^{3+}$ and $[Fe_4S_4]^{2+}$ respectively, were obtained using $[Fe(CN)_6]^{3-}$ as oxidant or ascorbate as reductant, followed by diafiltration. The u.v.–visible spectrum of the dark brown $Hipip_{ox}$ consists of a featureless absorption, increasing over the range 600—300 nm, whereas green $Hipip_{red}$ has a characteristic peak at 388 nm ($\varepsilon = 1.61 \times 10^4$ M^{-1} cm^{-1}),[1] as previously illustrated.[1,18] At 480 nm $Hipip_{ox}$ absorbs more strongly than $Hipip_{red}$, $\Delta\varepsilon = 1.0 \times 10^4$ M^{-1} cm^{-1}. Penta-ammine(aqua)-ruthenium(II) hexafluorophosphate, $[Ru(NH_3)_5(H_2O)][PF_6]_2$, was prepared as previously described,[23] and the composition confirmed by analysis. In a typical modification procedure $Hipip_{red}$ (17 mg, 0.18 mM) was reacted with $[Ru(NH_3)_5(H_2O)][PF_6]_2$ (35 mg, 7.0 mM) under argon (rigorous air-free conditions are required) in 20 mM hepes buffer, pH 7.5, for 45 min. The reaction was terminated by separating the protein from unreacted $[Ru(NH_3)_5(H_2O)]^{2+}$ using a Sephadex G25 gel column (3 × 25 cm), previously equilibrated with hepes buffer (20 mM, pH 7.5) under argon. The protein eluate was collected until the Ru band had moved *ca.* 80% down the column, and immediately oxidised with a slight excess of $[Fe(CN)_6]^{3-}$. The fully oxidised protein was dialysed into acetate buffer (20 mM, pH 5.2), and then loaded onto a CM52 cation-exchange column (1.5 × 20 cm) pre-equilibrated with the same buffer containing *ca.* 10 μM $[Fe(CN)_6]^{3-}$ to maintain the protein in the fully oxidised form. Elution was continued with this buffer at a flow rate of 2 cm^3 min^{-1} to provide effective chromatographic resolution of three (brown) bands. The first (*ca.* 10%) did not bind to the CM52 column, and had identical elution properties to native $Hipip_{ox}$ when chromatographed on DE52 cellulose columns. The second band (*ca.* 80%) eluted more slowly, and the third (*ca.* 10%) was much more strongly bound, but eluted rapidly in acetate (20 mM, pH 5.2) containing 0.1 M NaCl. The total protein recovery was 80% based on an ε for $Hipip_{ox}$ at 480 nm of 1.6×10^4 M^{-1} cm^{-1}. The major product was subjected to a series of characterisation experiments. The more strongly bound band, believed to be a more extensively modified fraction, was not further studied.

Analysis.—The Fe:Ru ratio was determined using inductively coupled plasma atomic emission spectrometry,[24] on a Bausch and Lomb ARL-2350 instrument, at the Johnson Matthey Technology Centre. From four determinations on two independently prepared samples the Fe:Ru ratio was found to be 3.99 ± 0.09, consistent with one Ru attached to the Hipip molecule.

U.v.–Visible Spectra.—These were recorded for $Hipip_{ox}$·Ru^{III} obtained by oxidation with excess $[Fe(CN)_6]^{3-}$ (410 mV),[25] and $Hipip_{red}$·Ru^{III}, obtained by reduction with excess of $[Co(terpy)_2]^{2+}$ (terpy = 2,2′:6′,2″-terpyridine) (260 mV).[26] The inorganic reagents were subsequently removed by diafiltration. In both cases spectra (250—700 nm) were as far as we could ascertain identical to those of $Hipip_{ox}$ and $Hipip_{red}$ respectively, and no contribution from the Ru^{III} was detected. The latter, attached to the protein as $Ru(NH_3)_5$(His), might be expected to contribute a peak at 303 nm (ε *ca.* 2 100 M^{-1} cm^{-1}).[27]

Diethyl Pyrocarbonate Modification.—Different behaviour was observed on addition of the histidine specific reagent diethyl pyrocarbonate (depc), $(C_2H_5OCO)_2O$ (Sigma Chemicals),[28] to native Hipip and Hipip·Ru^{III} (there was no dependence on the oxidation state of Hipip). With Hipip at pH 6.5 (0.10 M phosphate), the absorbance increase at 238 nm after 30 min for completion of the reaction (Figure 1), corresponded to 88% of the change expected for one histidine residue, based on the Δε for reaction with a free imidazole group (3 200 M^{-1} cm^{-1}).[28] Absorbance changes for *N*-ethoxyhistidine formation on a number of proteins have been found to be consistently 85 ± 3% of this value, yielding $\Delta\varepsilon = 2\,720 \pm 100$ M^{-1} cm^{-1}. However, no reaction was observed with Hipip·Ru^{III}.

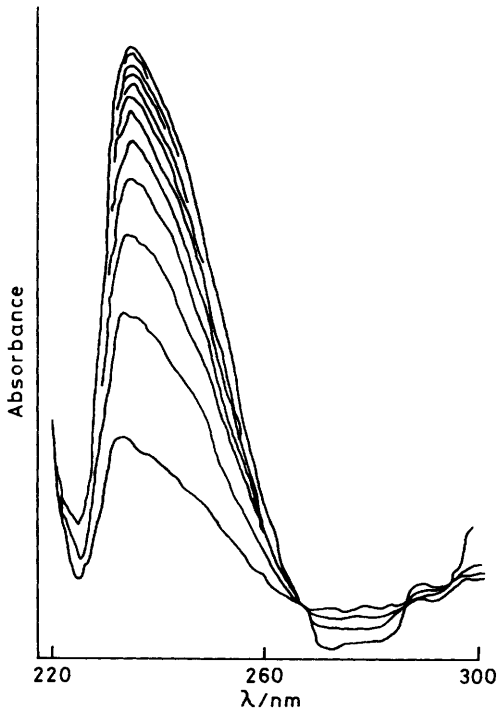

Figure 1. Reaction of native *C. vinosum* $Hipip_{red}$ (30 μM) with depc (20—30 fold excess), in 0.1 M phosphate buffer, pH 6.5, at 25 °C; repeat scans at 2 min intervals showing increase in absorbance at 238 nm. In a similar experiment with $Hipip_{ox}$·Ru^{III}, which was partly autoreduced to $Hipip_{red}$·Ru^{III}, no absorbance increase at 238 nm was observed

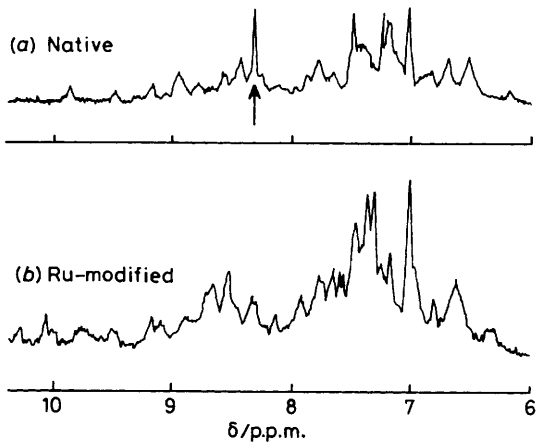

Figure 2. 300-MHz ^1H n.m.r. spectra (chemical shifts δ/p.p.m. from sodium 4,4-dimethyl-4-silapentanesulphonate) in the aromatic region for (*a*) native and (*b*) Ru^{III}-modified *C. vinosum* $Hipip_{red}$ in 0.10 M phosphate buffer at pH 7.0 (without correction for D_2O isotope effect). The sharp band at δ 8.3 p.p.m. in spectrum (*a*) is not observed in (*b*)

Proton N.M.R.—Spectra of solutions of native $Hipip_{red}$, $Hipip_{ox}$, $Hipip_{red}$·Ru^{III}, and $Hipip_{ox}$·Ru^{III}, exchanged into D_2O at pH 7.0 (0.10 M phosphate, uncorrected for the deuterium isotope effect), were obtained on a Bruker 300 MHz instrument, and referenced to the internal water signal at 4.8

Table 1. Comparison of contact-shifted resonances (δ/p.p.m.) in oxidised and reduced forms of native and Ru-modified *C. vinosum* Hipip

Resonance	$Hipip_{ox}$	$Hipip_{ox}$·Ru^{III}
C1	109.5	109.0
C2	39.0	38.0
C3	36.5	36.5
C4	30.0	29.0
C5	27.0	27.0
C6, C7	26.5, 15.0	24.5, 24.0
C8	−36	−34.5
C9	−37.5	−35.5
	—	−3.5
	$Hipip_{red}$	$Hipip_{red}$·Ru^{III}
CI	16.5	16.3
CII	15.9	15.9
CIII	12.6	12.8
	—	−3.5

p.p.m. The ^1H n.m.r. spectra of native $Hipip_{red}$ (diamagnetic) and $Hipip_{red}$·Ru^{III} in the aromatic region are compared in Figure 2. Disappearance of the previously assigned [15] resonance at 8.3 p.p.m. is the most notable result of $Ru^{III}(t_{2g}^5)$ attachment. Shifts of other resonances in the more complex 7.0—7.5 p.p.m. region are also observed.

Spectra were also recorded over a wider chemical shift range, when contact shifted resonances resulting from the paramagnetism of the $[Fe_4S_4]^{3+}$ centre were observed. Nine resonances in *C. vinosum* $Hipip_{ox}$ attributed to individually unassigned $C_\beta H$ and $C_\alpha H$ protons of the four cysteinyl residues have been noted.[15] A comparison of the contact shift pattern with $Hipip_{ox}$·Ru^{III} is given in Table 1 indicating a high degree of correlation. Only resonances C6 and C7 appear to have been perturbed.[15] The contact shifts CI, CII, and CIII in the spectra of $Hipip_{red}$ and $Hipip_{red}$·Ru^{III} are indistinguishable.[15] An additional peak at *ca.* −3.5 p.p.m. was observed for both $Hipip_{ox}$·Ru^{III} and $Hipip_{red}$·Ru^{III}, which it has not so far been possible to assign.

Reduction Potential.—This was determined for the $[Fe_4S_4]^{3+/2+}$ centre in Ru-modified Hipip by spectrophotometric titration with $[Fe(CN)_6]^{4-}$. To three 1 cm^3 solutions of fully oxidised $Hipip_{ox}$·Ru^{III} in 0.10 M phosphate buffer (pH 7.0), were added 0, 2.0, and 3.0 cm^3 of $[Fe(CN)_6]^{4-}$ (0.93 mM) in the same buffer. The volume of each solution was adjusted to 5.0 cm^3 with buffer to give a final protein concentration of 18.2 μM. From absorbance readings at 480 nm, assuming absorption coefficients for $Hipip_{ox}$·Ru^{III} (1.6×10^4 M^{-1} cm^{-1}) and $Hipip_{red}$·Ru^{III} (6.0×10^3 M^{-1} cm^{-1}) are the same as for unmodified protein, the equilibrium constant K was calculated. Using the Nernst equation, and a value of 410 mV (*vs.* normal hydrogen electrode, n.h.e.) for $[Fe(CN)_6]^{3-/4-}$, a reduction potential of 350 ± 10 mV (*vs.* n.h.e.) was obtained. The separation in $[Fe(CN)_6]^{3-/4-}$ and $[Ru(NH_3)_5(His)]^{3+/2+}$ reduction potentials is sufficiently large (270 mV)[29] to assume that negligible Ru^{II} is produced.

Stability.—At an early stage in this work it was observed from absorbance changes that slow reduction of $Hipip_{ox}$·Ru^{III} to $Hipip_{red}$·Ru^{III} occurred, and that this was enhanced by bubbling argon gas through solutions (a procedure which is necessary prior to pulse radiolysis studies). The precise nature of this 'autoreduction' process has not been established. It does not correspond to protein denaturation since re-oxidation (followed by further autoreduction) is possible. The effect was quantified

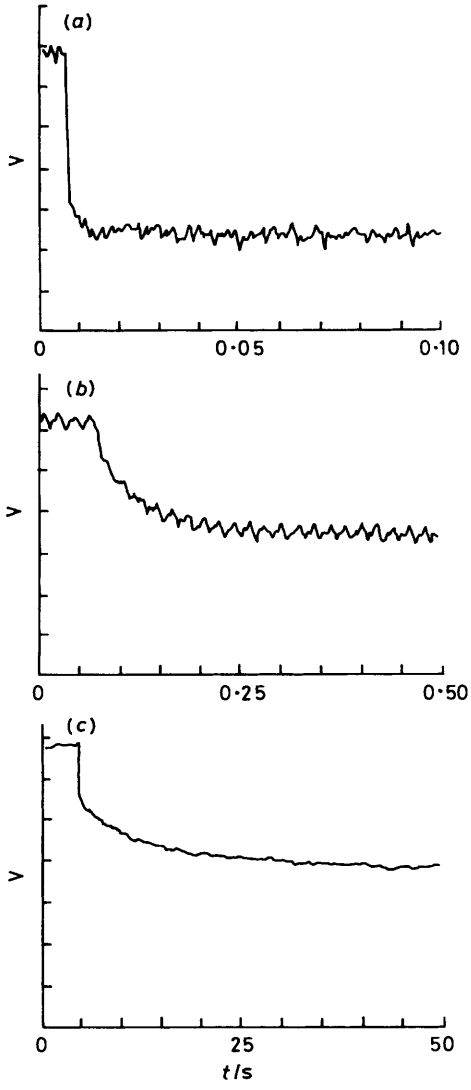

Figure 3. Pulse radiolysis experiments (not same dosage) with e_{aq}^- as reductant monitored at 480 nm, solutions in 0.10 M phosphate (pH 7.0), 20 °C. (*a*) Stage 1, with native Hipip (10 μM), full-scale time-base 0.10 s, absorbance $\Delta A = 0.0032$ per division (here indicated by photomultiplier voltage V), with no subsequent changes over >20 s. (*b*) Stage 2, $Hipip_{ox}$·Ru^{III} (2.0 μM), full-scale time-base 0.5 s, $\Delta A = 0.0019$ per division (first pulse). (*c*) Stage 3, $Hipip_{ox}$·Ru^{III} (3.9 μM), full-scale time-base 50 s, $\Delta A = 0.0047$ per division (first pulse)

for a 40 μM $Hipip_{ox}$·Ru^{III} solution in 0.10 M phosphate buffer at pH 7.0 (12 cm^3). Argon (high purity, B.O.C.) at a flow rate of 6.5 cm^3 min^{-1} (*via* 0.5 mm Teflon tubing) was bubbled through the solution, and at 5 min intervals 1 cm^3 was removed and the u.v.–visible spectrum determined. After 1 h, 58% reduction to $Hipip_{red}$·Ru^{III} was observed, and after 2 h reduction was essentially complete in what appeared to be a zero-order process with respect to protein concentration. A similar experiment with native $Hipip_{ox}$ at pH 7.0 produced no detectable reduction and at pH 4.5 (0.01 M acetate buffer), when His 42 will be protonated, only 10% reduction was observed in 45 min.

Pulse Radiolysis Studies.—These were carried out at the Cookridge Radiation Research Centre using established procedures.[30] A 5-cm path length reaction cell was used; the temperature was 19.0 ± 1.5 °C. Reduction of native $Hipip_{ox}$ was

achieved using the hydrated electron (e^-_{aq}), and that of $Hipip_{ox}$·Ru^{III} using e^-_{aq}, the formate radical ($CO_2^{\bullet -}$), and superoxide (O_2^-). The yield of reducing radical produced for a given dose was determined by thiocyanate dosimetry.[31] Radiation doses were chosen such that less than 20% of the total Hipip was reduced on each pulse. Solutions of protein (1—4 μM), first $Hipip_{ox}$ and then $Hipip_{ox}$·Ru^{III}, in 0.10 M phosphate buffer (pH 7.0), containing the required radical scavenging species, were prepared for pulse radiolysis by saturation with the required gas, which entered through a fine sinter. To obtain e^-_{aq}, argon saturated solutions, containing 0.40 M 2-methylpropan-2-ol (B.D.H., AnalaR) to scavenge OH and H, were used. For $CO_2^{\bullet -}$ radicals, N_2O saturated solutions ($e^-_{aq} + N_2O + H_2O \longrightarrow N_2 + OH + OH^-$), containing 0.10 M sodium formate (B.D.H. or Merck Pro anal.) to convert both OH and H to the reducing radical $CO_2^{\bullet -}$, were used. For O_2^- the procedure was as for $CO_2^{\bullet -}$, but solutions were in this case saturated with O_2 ($CO_2^{\bullet -}$ and e^-_{aq} react with O_2 to give O_2^-). Reactions were monitored at 480 nm.

It was necessary to establish the extent of reduction of $Hipip_{ox}$·Ru^{III} which occurred when solutions were flushed with argon for 10—15 min prior to pulsing. This was done by comparing the absorbance at 480 nm in the same 5 cm cell before and after solutions were reduced (by pulse radiolysis) to the $Hipip_{red}$·Ru^{III} state.

Stopped-flow Studies.—The reaction (25 °C) of $Hipip_{red}$·Ru^{II} (46 μM) with $Hipip_{ox}$·Ru^{III} (*ca.* 5 μM) in 0.10 M phosphate (pH 7.0) was monitored at 480 nm. Fully reduced protein was prepared by reduction with excess ascorbate, followed by diafiltration under argon.

Complexes.—The bis(2,2′:6′,2″-terpyridine)cobalt(II) perchlorate monohydrate complex (ligand from Sigma Chemicals) was prepared and purified to the known visible spectrum: λ 445 (ε 1 620) and 505 nm (1 420 M^{-1} cm^{-1}).[26] Commercial potassium hexacyanoferrate(III) (B.D.H., AnalaR) was used without further purification: λ 300 (ε 1 600) and 420 nm (1 010 M^{-1} cm^{-1}).

Buffers.—Dipotassium hydrogenphosphate and potassium dihydrogenphosphate salts (B.D.H., AnalaR) were used for buffering at pH 7.0, and in some experiments *N*-2-hydroxyethylpiperazine-*N*′-2-ethanesulphonic acid, hepes (Sigma Chemicals) was used.

Analysis of Data.—Pulse radiolysis absorbance (A) plots of $-\ln (A_t - A_\infty)/(A_0 - A_\infty)$ against time were linear to 3.5 half-lives unless otherwise stated, and rate constants were obtained from a weighted linear regression method. Use of the Guggenheim method[32] gave rate constants in satisfactory agreement with those obtained using measured A_∞ values.

Results

Three distinct kinetic stages are observed at 480 nm for the reaction of e^-_{aq} with $Hipip_{ox}$·Ru^{III}. After the initial rapid reaction (stage 1), two further well separated stages (2 and 3) are observed. Figure 3(*b*) and (*c*) illustrate the latter, and Figure 3(*a*) (with an extended time-base) clearly indicates that stage 2 is absent for native $Hipip_{ox}$. The rate constant (k_1) for the reaction of $Hipip_{ox}$ with e^-_{aq} has been determined previously,[33] and is 1.7×10^{10} M^{-1} s^{-1}. For the concentrations used in the present work (2 μM $Hipip_{ox}$, 0.5 μM e^-_{aq}) the reaction was complete in < 200 μs, and thus appeared as a step on the time-scale of 50 ms per division.

For stage 2, seen only with Ru-modified Hipip, a plot of $-\ln (A_t - A_\infty)/(A_0 - A_\infty)$ against time is shown in Figure 4.

Table 2. Pulse radiolysis studies using e^-_{aq} as reductant for $Hipip_{ox}$·Ru^{III}. Rate constants (~20 °C) for stage 2 assigned to intramolecular electron transfer of $Hipip_{ox}$·Ru^{II} in 0.10 M phosphate (pH 7.0). Runs indicated are for successive pulses of one solution

$10^6[Hipip\text{-}Ru]_T$*/M	$10^6[Hipip_{ox}\text{-}Ru^{III}]$/M	$k_{obs.}/s^{-1}$
2.0	0.64	18.8
2.0	0.36	23.6
2.0	0.18	19.2
2.0	0.70	16.3
2.0	0.33	18.1
2.0	0.71	17.6
2.0	0.50	15.0
3.9	1.58	19.1
3.9	1.58	18.8
3.9	0.93	20.1
3.9	1.83	20.5
3.9	1.01	18.9
1.7	0.76	19.8
1.7	0.46	14.8
1.7	0.60	15.3
1.7	0.30	13.4
1.7	0.13	13.6
1.7	0.59	14.8
1.7	0.35	15.7
1.7	0.14	18.7
1.7	0.65	18.0

* Total concentration of modified protein.

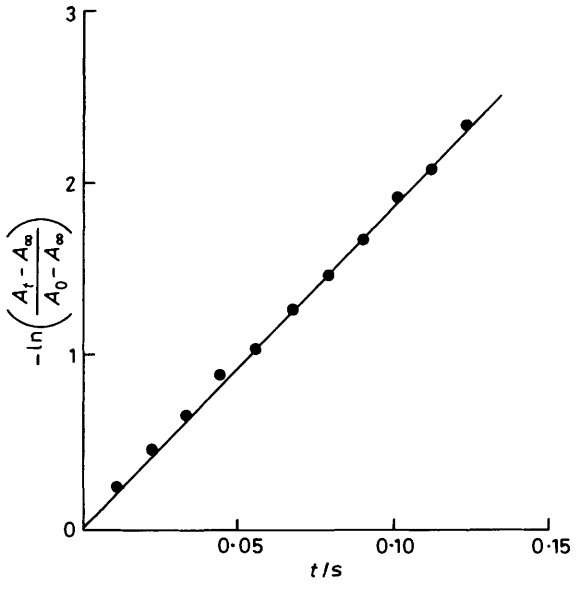

Figure 4. Pulse radiolysis of $Hipip_{ox}$·Ru^{III}; first-order plot for stage 2, corresponding to intramolecular electron transfer of $Hipip_{ox}$·Ru^{II}. This plot corresponds to the first entry in Table 2

Rate constants obtained from such plots are listed in Table 2. Concentrations of $Hipip_{ox}$·Ru^{III} remaining after argon bubbling were determined from the initial absorbance.

Variation of $Hipip_{ox}$·Ru^{III} concentrations (two-fold by dilution and ten-fold by successive pulsing) did not affect the observed rate constant, $k_2 = 18 \pm 2$ s^{-1} at 20 °C. This stage is assigned to the intramolecular process (1). From a consider-

$$Hipip_{ox}\text{·}Ru^{II} \longrightarrow Hipip_{red}\text{·}Ru^{III} \quad (1)$$

ation of the $[Fe_4S_4]^{3+/2+}$ and $[Ru(NH_3)_5(His)]^{3+/2+}$ (*ca.* 80 mV) reduction potentials $Hipip_{red}$·Ru^{III} is a stable state. There

Table 3. Reaction of $e_{aq.}^-$, $CO_2^{\bullet -}$, and O_2^- with $Hipip_{ox}$·Ru^{III} in the presence of $[Fe(CN)_6]^{3-}$. Rate constants (*ca.* 20 °C) for stage 2 assigned to intramolecular electron transfer of $Hipip_{ox}$·Ru^{II}, in 0.10 M phosphate (pH 7.0)

Reductant	10^6[$Hipip_{ox}$·Ru^{III}]/M	$k_{obs.}/s^{-1}$
e^-_{aq}	1.60	19.4
	1.60	19.6
	1.60	16.9
$CO_2^{\bullet -}$	1.70	23.7
	0.90	19.4
	0.90	18.9
O_2^-	0.90	14.2
	0.90	15.0
	0.90	17.1
	0.90	17.0
	0.90	17.0
	0.90	19.2

Table 4. Stopped-flow absorbance changes (ΔA) and rate constants $k_{obs.}$ (25 °C), for the reaction of $Hipip_{ox}$·Ru^{III} (≈ 5 μM) with $Hipip_{red}$·Ru^{II} (46 μm) in 0.10 M phosphate (pH 7.0)

$10^2\Delta A$	$k_{obs.}/s^{-1}$	$10^4k/M^{-1}$ s^{-1}
4.3	1.11	0.49
3.7	0.56	1.21
5.4	0.49	1.07
4.1	0.57	1.24
4.6	0.55	1.20

was no evidence for contributions from bimolecular processes on this time-scale.

Stage 3 was observed on a time-scale of 5—10 s per division. It is associated with the presence of $Hipip_{red}$·Ru^{III} resulting from the autoreduction process accelerated by gas bubbling. Only *ca.* 40% of the $Hipip_{ox}$·Ru^{III} remains after bubbling argon and before the first electron pulse on this time-scale. It was noted that the fraction of reduction occurring in stage 3 increased with consecutive pulsing of the solution, while the fraction of reduction occurring in stages 1 and 2 both decreased. In other words stage 3 becomes increasingly important as the pre-pulse concentration of $Hipip_{red}$·Ru^{III} increases, and that of $Hipip_{ox}$·Ru^{III} decreases. Here we assign stage 3 to equation (2),

$$Hipip_{red}\text{·}Ru^{II} + Hipip_{ox}\text{·}Ru^{III} \longrightarrow 2\ Hipip_{red}\text{·}Ru^{III} \quad (2)$$

consistent with the various experimental observations. Concentrations of the reactants in equation (2) are not as required for pseudo-first-order kinetics, and first-order kinetic plots were in many cases linear to only *ca.* 50% completion. From initial slopes rate constants in the range $k_3' = 0.05$—$0.5\ s^{-1}$ were indicated. An estimated second-order rate constant for stage 3 is therefore $k_3 \approx 1 \times 10^5\ M^{-1}\ s^{-1}$.

In order to prevent $Hipip_{red}$·Ru^{II} formation by re-oxidising $Hipip_{red}$·Ru^{III} as it is generated in the bubbling stage, a 2—5 fold molar excess of $[Fe(CN)_6]^{3-}$ was added initially. Both $[Fe(CN)_6]^{3-}$ and $[Fe(CN)_6]^{4-}$ have negligible absorbance at 480 nm. Under these conditions, with e^-_{aq} as reductant, no stage 3 was obtained. On completion of stage 2 (k_2 in Table 3), an upward drift in absorbance was observed, Figure 5(*a*), resulting from the re-oxidation of $Hipip_{red}$·Ru^{III} by $[Fe(CN)_6]^{3-}$. If the solution is continuously pulsed until all the $[Fe(CN)_6]^{3-}$ is reduced, then in subsequent pulses some contribution to the absorbance change ΔA_{480} from stage 3 reappears.

An additional experiment was carried out, to see whether super-reduced Hipip, the $[Fe_4S_4]^+$ state, might be formed on

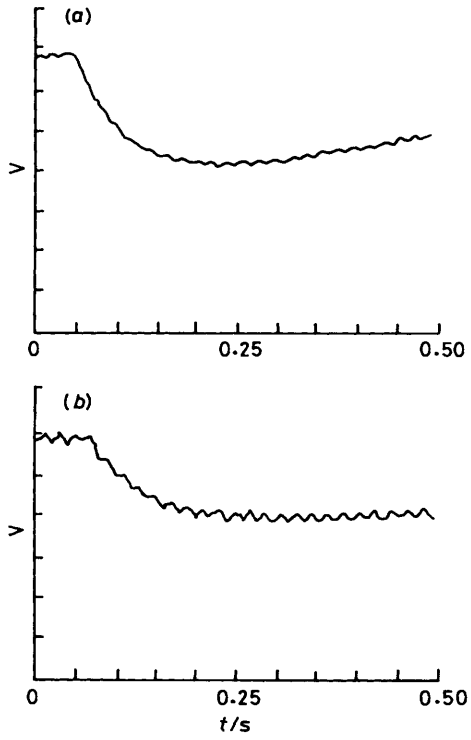

Figure 5. Pulse radiolysis of $Hipip_{ox}$·Ru^{III} in the presence of $[Fe(CN)_6]^{3-}$ in 0.1 M phosphate (pH 7.0), *ca.* 20 °C. (*a*) With e^-_{aq} as reductant and 1.6 μM protein, 4 μM $[Fe(CN)_6]^{3-}$; (*b*) O_2^- as reductant, 0.90 μM protein, 20 μM $[Fe(CN)_6]^{3-}$. In (*a*) stage 2 is followed by $[Fe(CN)_6]^{3-}$ re-oxidation of the $Hipip_{red}$ state. A similar stage is observed in (*b*) when sufficient $[Fe(CN)_6]^{3-}$ is present

pulsing a solution initially in the $Hipip_{red}$·Ru^{III} state. On the same time-scale as stage 2 no reaction with e^-_{aq} was detected at 410 nm, the wavelength giving the largest absorbance change for this process.[33] Therefore e^-_{aq} reacts preferentially with Ru^{III}. After several pulses, as $Hipip_{red}$·Ru^{II} accumulates, a signal did in fact appear on the time-scale of 0.2 s per division. Rapid reduction was followed by a slower reoxidation (the process observed) consistent with the formation of $Hipip_{s\text{-}red}$·Ru^{II} and its re-oxidation to $Hipip_{red}$·Ru^{II}. The rate constant for the latter (~1.5 s^{-1}) is in close agreement with the value previously reported for the decay of $Hipip_{s\text{-}red}$ generated in pulse radiolysis studies.[34] This would seem to preclude the possibility that $Hipip_{s\text{-}red}$·Ru^{II} formation is an alternative explanation to equation (2).

In further studies the $CO_2^{\bullet -}$ radical and O_2^- were generated instead of e^-_{aq} in pulse radiolysis procedures, and reacted with $Hipip_{ox}$·Ru^{III}. Solutions prepared by bubbling N_2O or O_2 (as described in the Experimental section) also gave $Hipip_{red}$·Ru^{III} in an autoreduction process, as observed with argon. Therefore $[Fe(CN)_6]^{3-}$ (10 — 20 μM) was added to maintain the fully oxidised state during bubbling. A typical trace for stage 2 after reaction with O_2^- is shown in Figure 5(*b*). Rate constants for stage 2 are as listed in Table 3. Similar traces were observed for $CO_2^{\bullet -}$ where if sufficient $[Fe(CN)_6]^{3-}$ is present re-oxidation is observed as in Figure 5(*a*). Again no stage 3 (k_3) was observed. Rate constants k_2 are in close agreement with those obtained in the e^-_{aq} studies, Table 3.

Finally with regard to the feasibility of equation (2) the reaction of $Hipip_{red}$·Ru^{II} (46 μM) with $Hipip_{ox}$·Ru^{III} (~5 μM) was studied by conventional stopped-flow spectrophotometry at 480 nm. Absorbance changes observed were consistent with equation (2). Rate constants (25 °C) obtained are listed in Table 4.

Discussion

The reaction of *C. vinosum* Hipip with $[Ru(NH_3)_5(H_2O)]^{2+}$ occurs readily under conditions which have been shown to favour ruthenium modification of other metalloproteins.[34–40] A product containing one Ru per molecule is obtained in *ca.* 80% yield. The ease with which Hipip is modified, compared with *e.g.* cytochrome c, reflects the electrostatic attraction of $[Ru(NH_3)_5(H_2O)]^{2+}$ for the protein, estimated charge −4 for $Hipip_{red}$ at neutral pH. Oxidation with $[Fe(CN)_6]^{3-}$ yields the fully oxidised Ru^{III} product as $Hipip_{ox}$·Ru^{III}.

A comparison of the reactivity of native $Hipip_{ox}$ and $Hipip_{ox}$·Ru^{III} towards depc allows the site of modification to be specified. Since there is only one histidine residue in *C. vinosum* Hipip, the absorbance increase observed at 238 nm for native Hipip can be unambiguously assigned to the reaction of depc at His 42, Figure 1. The modified protein $Hipip_{ox}$·Ru^{III} shows no reaction with depc, which demonstrates that in a singly modified Hipip, His 42 is the exclusive site of modification. Attachment of the Ru at the N^{ε} of the imidazole ring is most likely.

The C_2H and C_4H ^1H n.m.r. resonances of His 42 in *C. vinosum* Hipip have been assigned previously.[15] At pH 7.0, for $Hipip_{red}$, they appear at δ 8.3 and 7.3 p.p.m. respectively. In Figure 2, a sharp C_2H proton signal at δ 8.3 p.p.m. is present in native $Hipip_{red}$, but is absent in $Hipip_{red}$·Ru^{III}. The paramagnetic Ru^{III} centre is believed to have shifted and broadened the resonances of adjacent protons due to electron-nuclear dipolar relaxation.[14] Disappearance of the C_2H resonance is consistent with assignment of His 42 as the Ru-binding site. Because of the complexity of the spectrum for native $Hipip_{red}$ in the δ 7—7.5 region the C_4H resonance could not be unambiguously assigned. This region has undergone some changes in modified Hipip.

Three lines of evidence suggest that the Fe_4S_4 centre of the Ru-modified protein is essentially unperturbed by modification. First, u.v.–visible spectra for native and modified proteins in the same oxidation state are virtually indistinguishable. In addition to implying that the electronic properties of the cluster have not been drastically affected, this observation is important because it allows the previously reported absorption coefficients for the native protein to be used for the modified species. Secondly, a more sensitive probe of the active site is found in the ^1H n.m.r. contact-shift resonances. Contact-shift spectra for four species of Hipip have been published,[15,16] and each shows a quite individual shift pattern. The pattern observed may be viewed as characteristic of the electron distribution within the cluster. Spin-density distribution on the cysteine ligands is expected to depend on their immediate chemical environment, and to be quite susceptible to conformational and electrostatic effects. Because His 42 is adjacent to Cys 43 and only 8 Å from the Fe_4S_4 core, some perturbation of the Cys 43 $C_\beta H$ resonances is to be expected. These resonances are tentatively assigned as C6 and C7 in Table 1. The agreement of other contact shifts for native and Ru-modified proteins is extremely good, implying little or no rearrangement of the active site on Ru-modification. The third piece of evidence against active site perturbation is the $[Fe_4S_4]^{3+/2+}$ reduction potential for the Ru-modified protein. The value of 350 ± 10 mV (*vs.* n.h.e.) is the same as that found for native Hipip at pH 7.[21] Determination of the $[Ru(NH_3)_5(His)]^{3+/2+}$ couple for other modified proteins has demonstrated that the reduction potential does not change by more than 50 mV from that for the unattached Ru couple.

An unexpected and extraordinary property of $Hipip_{ox}$·Ru^{III} is its ability to undergo reduction at the $[Fe_4S_4]^{3+}$ centre without addition of an external reductant. The phenomenon does not occur solely by bubbling gas through solutions of $Hipip_{ox}$·Ru^{III}. It has been observed after thawing frozen samples stored in the dark for several days, and also by passing a fully oxidised sample down a DE52 anion-exchange column under conditions of weak binding. It is important to note that the cycle of autoreduction and re-oxidation can be repeated several times. The process may correspond to some form of surface or catalysed reduction, or some process resulting from the agitation of solutions. One possibility requires the existence of a protein conformation which exposes the cluster to solvent. Since the $[Fe_4S_4]^{3+}$ state is not observed with ferredoxins which have solvent-exposed clusters,[8] the driving force for formation of $[Fe_4S_4]^{2+}$ could become large, and possibly greater than the *ca.* 0.9 V required to oxidise water at pH 7.[41] This conformation is presumably not present for native $Hipip_{ox}$, but Ru-modification could lower the energy barrier sufficiently for it to become accessible.

Discussion of the pulse radiolysis studies on Ru-modified Hipip requires consideration of different stages of reaction. The rapid reduction of $Hipip_{ox}$·Ru^{III} by e^-_{aq}, $CO_2^{\bullet -}$, and O_2^- (stage 1) may occur at either the $[Fe_4S_4]^{3+}$ or the Ru^{III} site, as indicated in equation (3). Reduction of the $[Fe_4S_4]^{3+}$ centre of

$$e^-_{aq} + Hipip_{ox}\cdot Ru^{III} \begin{array}{l} \nearrow\ Hipip_{ox}\cdot Ru^{II} \\ \searrow\ Hipip_{red}\cdot Ru^{III} \end{array} \qquad (3)$$

$Hipip_{ox}$ is monitored at 480 nm. Since stages 2 and 3 are not observed in the reduction of native $Hipip_{ox}$, their observation with Ru-modified Hipip must result from processes following the initial reduction of Ru^{III}. Selectivity between the two paths in equation (3) varies with the nature of the reducing radical. Because of the 'buried' nature of the Hipip active site, its reduction by $CO_2^{\bullet -}$ and O_2^- is more difficult to achieve than with e^-_{aq}, which can gain access to the cluster more readily. This is supported by the observation that super-reduced Hipip is not obtained by the action of strong reducing agents such as $[Cr(edta)]^{2-}$ (−1.0 V; edta = ethylenediamine-*NNN'N'*-tetra-acetate) on $Hipip_{red}$,[42] but is produced on reduction with e^-_{aq}.[33] The selectivity of $[Fe_4S_4]^{3+}$ over Ru^{III} is virtually zero with $CO_2^{\bullet -}$ and O_2^-, and reduction occurs exclusively at the Ru^{III} rather than $[Fe_4S_4]^{3+}$. With e^-_{aq} the selectivity is dependent on the extent of reduction of the sample. A selectivity of $[Fe_4S_4]^{3+}$ to Ru^{III} above 0.3 was not observed in this work, but significantly higher values would be expected if the sample was initially fully oxidised.

Of the two semireduced species generated in stage 1, $Hipip_{red}$·Ru^{III} is the thermodynamically stable form. Under conditions where only a small fraction of the total protein (<20%) is reduced in one pulse, the transient species $Hipip_{ox}$·Ru^{II} can decay to $Hipip_{red}$·Ru^{III} by two possible paths, equations (4) and (5). There are two reasons for believing that

$$Hipip_{ox}\cdot Ru^{II} \longrightarrow Hipip_{red}\cdot Ru^{III} \qquad (4)$$

$$Hipip_{ox}\cdot Ru^{II} + Hipip_{ox}\cdot Ru^{III} \longrightarrow Hipip_{ox}\cdot Ru^{III} + Hipip_{red}\cdot Ru^{III} \qquad (5)$$

the intramolecular process (4) is dominant. First, the rate constant k_2 is independent of the concentration of $Hipip_{ox}$·Ru^{III} (in the range 0.13—1.83 μM) used. Secondly, the decay remains first order after several pulses, when $Hipip_{ox}$·Ru^{III} is sufficiently depleted for pseudo-first-order conditions no longer to apply in equation (5). The rate constant for stage 2 is not affected by choice of reductant or the presence of a small excess of $[Fe(CN)_6]^{3-}$. It has also been established that the formation of super-reduced Hipip is not an important contributing factor.

Stage 3 is now considered. If this stage gave consistently first-order behaviour then a reasonable explanation would be slow intramolecular electron transfer, possibly following the trapping

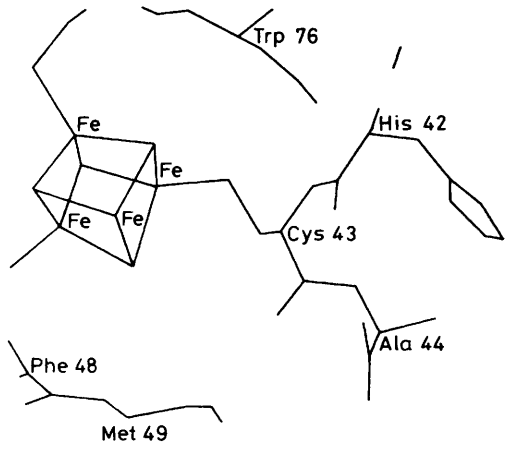

Figure 6. The Fe_4S_4 active site of Hipip, which is co-ordinated by Cys 43, and the position of His 42 which is Ru-modified, obtained from crystal structure information (Brookhaven Data Base, refs. 6 and 7), using Evans and Sutherland computer graphics

of an electron at a site on the protein surface. On the first pulse the behaviour observed would be the same as for stage 2. However, the increase in magnitude of stage 3 relative to stages 1 and 2 on successive pulsing cannot reasonably be accounted for by such an explanation. As a result of autoreduction the concentration of $Hipip_{red}\cdot Ru^{III}$ in these experiments is at least as high as that of $Hipip_{ox}\cdot Ru^{III}$. Thus bearing in mind the selectivity in favour of reduction at Ru^{III}, significant amounts of the doubly reduced species $Hipip_{red}\cdot Ru^{II}$ will be produced on pulsing. With doubly oxidised $Hipip_{ox}\cdot Ru^{III}$ still present, equation (6) becomes a

$$Hipip_{ox}\cdot Ru^{III} + Hipip_{red}\cdot Ru^{II} \xrightarrow{k_3} 2\ Hipip_{red}\cdot Ru^{III} \quad (6)$$

reasonable explanation for stage 3. Consistent with such a reaction a net absorbance decrease is observed at 480 nm. As the concentration of $Hipip_{ox}\cdot Ru^{III}$ is depleted by continued pulsing and conditions arise where the excess (never more than eight-fold) over $Hipip_{red}\cdot Ru^{II}$ becomes even less, the approximation to pseudo-first-order behaviour (which applies for the first pulse) breaks down completely.

The reaction proposed in equation (6) has been studied by the stopped-flow method, and a rate constant of $1.2 \times 10^4\ M^{-1}\ s^{-1}$ obtained. Experimental conditions were as close as possible to those used in pulse radiolysis experiments, with absorbance changes (≈ 0.04) small for stopped-flow studies. The rate constant obtained is about eight times slower than that observed for k_3 by pulse radiolysis ($\approx 10^5\ M^{-1}\ s^{-1}$). The latter is approximate however, because precise concentrations of reactants were not known. Also there is no way of ensuring that, at the concentration levels used in the stopped-flow studies, the Ru^{II} state is retained. Given these uncertainties it is reasonable to conclude that equation (6) contributes to stage 3.

For intramolecular electron transfer in stage 2 the shortest through-space distance (d) between the two redox centres is estimated from molecular graphics to be 7.9 ± 0.3 Å, corresponding to the distance of C^{γ} of His 42 to the nearest μ_3-S of the Fe_4S_4 core. It is possible that this distance changes on modification, although from the studies here described there is no evidence for large conformational changes in the region of the Fe_4S_4 core. The through-bond distance (Figure 6) is estimated to be *ca.* 13 Å, which is much shorter than any comparable distance in other Ru-modified metalloproteins to date. For example, with horse-heart cytochrome c modified at His 33 (rate constants 30 and 53 s^{-1} from two independent studies)[36,37] and *P. aeruginosa* azurin modified at His 83 (rate constant 1.9 s^{-1}),[38,39] the shortest polypeptide connection between donor and acceptor sites is > 100 Å. A contribution to electron transfer from a through-bond process in $Hipip_{ox}\cdot Ru^{II}$ cannot therefore be discounted. Theoretical considerations[43] indicate that through-bond transfer (as opposed to through space) may be more efficient in some instances. If such a mechanism is operative in $Hipip_{ox}\cdot Ru^{II}$, it is not reflected in a significant enhancement in the rate constant when compared to the above systems.

It is interesting to compare the intramolecular rate constant for His 42-modified Hipip at 18 s^{-1} (d = 7.9 Å), with that of His 33-modified cytochrome c at 30 or 53 s^{-1} (d = 11.8 Å). Electron transfer in the latter case is apparently faster despite the greater redox centre separation d. In cases of weak donor–acceptor coupling (non-adiabatic electron transfer) it has been proposed that the electron-transfer rate decreases exponentially with distance[44] according to equation (7). Here, k_0 is the rate

$$k_{obs.} = k_0 \exp(-\beta d) \quad (7)$$

constant for electron transfer in the hypothetical instance where $d \approx 4$ Å (van der Waals contact), and β is the transmission coefficient, a measure of the strength of donor–acceptor coupling. A correlation of $\ln k_{obs.}$ *vs.* d has been made[45] for three intramolecular electron-transfer reactions in which horse-heart cytochrome c is the acceptor. Values of k_0 of $6 \times 10^4\ s^{-1}$, and $\beta = 0.9\ Å^{-1}$ have been obtained. Since the intramolecular driving force for $Hipip_{ox}\cdot Ru^{II}$ (~ 0.27 V) is similar to that for the other examples considered (0.19, 0.40, and 0.26 V respectively), it is worthwhile drawing a comparison. If the quoted values of k_0 and β (with cytochrome c as acceptor) are applied in the Hipip case, then the rate constant of 18 s^{-1} is about two orders of magnitude smaller than expected.

Several factors may contribute to this unexpectedly small intramolecular rate constant. The Fe_4S_4 site is quite different from the above haem systems, and may have intrinsically weaker donor–acceptor capabilities (larger β values). Also the activation barrier for intramolecular transfer in $Hipip_{ox}\cdot Ru^{II}$ may be significantly higher than in the cytochrome c reactions, leading to a smaller value for k_0. Another factor which cannot be ignored is the effect of intervening medium on donor–acceptor coupling. Indeed, studies involving *A. variabilis* and *S. obliquus* plastocyanin suggest that the intervening medium is of crucial importance.[40] Thus $Ru(NH_3)_5^{2+}$ attached at His 59 does not provide a favourable location for electron transfer ($< 0.26\ s^{-1}$) to the Cu^{II} active site (11.9 Å). Quite remarkably, when in the case of native *S. obliquus* plastocyanins, $[Ru(NH_3)_5(C_3H_4N_2)]^{2+}$ ($C_3H_4N_2$ = imidazole), as reductant, is unattached and allowed to select a site for reaction, a very fast electron-transfer process ($> 5 \times 10^3\ s^{-1}$) ensues, even though the predominant reaction site (the negative patch) is further away from the Cu. We note that residue 42 on this negative patch is connected directly to the Cu active site (His 37 is ligated), as is nearby Phe 83 (Cys 84 is ligated). However on the evidence of the present Hipip studies there is no reason for supposing that such direct links are relevant, unless it is that in combination they provide some sort of channel assisting electron transfer.

Site-directed mutagenesis, where individual amino acids can be replaced and tested in turn for their effect on reactivity, is the most direct way in which influence of specific residues (for example aromatics) on the protein can be further assessed in the context of intramolecular electron transfer.

Acknowledgements

We are most grateful to Johnson Matthey for a C.A.S.E. award with the S.E.R.C. (to M. P. J.) and for the loan of Ru. We

particularly wish to thank Dr. D. T. Thompson at the Johnson Matthey Technical Centre for his enthusiastic support of this work. We also wish to acknowledge the help of Drs. J. G. Vinter and M. R. Saunders of Smith Kline and French for their generous help and use of computer graphics facilities. M-C. L. was on leave from the University of Malaya, Kuala Lumpur, Malaysia.

References

1 R. G. Bartsch, *Methods Enzymol.*, 1971, **23**, 644 and refs. therein.
2 K. Dus, S. M. Tedro, and R. G. Bartsch, *J. Biol. Chem.*, 1973, **248**, 7318; S. M. Tedro, T. E. Meyer, R. G. Bartsch, and M. D. Kamen, *J. Biol. Chem.*, 1981, **256**, 731.
3 S. M. Tedro, T. E. Meyer, R. G. Bartsch, and M. D. Kamen, *J. Biol. Chem.*, 1981, **256**, 731.
4 See, for example, R. E. Dickerson, in 'The Chemical Basis of Life,' Scientific American Inc., 1973, pp. 82—95; *Sci. Am.*, 1972, **226**, 58.
5 See, for example, J. A. M. Ramshaw, in 'Nucleic Acids and Proteins in Plants I, Encyclopedia of Plant Physiology,' eds. D. Boulter and B. Parthier, Springer Verlag, Berlin, 1982, vol. 14A, pp. 229—240; M. P. Jackman, J. D. Sinclair-Day, M. J. Sisley, A. G. Sykes, L. A. Denys, and P. E. Wright, *J. Am. Chem. Soc.*, 1987, **109**, 6443.
6 C. W. Carter jun., J. Kraut, S. T. Freer, N.-H. Xuong, R. A. Alden, and R. G. Bartsch, *J. Biol. Chem.*, 1974, **249**, 4212.
7 C. W. Carter jun., J. Kraut, S. T. Frier, and R. A. Alden, *J. Biol. Chem.*, 1974, **249**, 6339.
8 L. C. Sieker, E. T. Adman, and L. H. Jensen, *Nature (London)*, 1972, **235**, 40.
9 C. W. Carter jun., J. Kraut, S. T. Freer, R. A. Alden, L. C. Sieker, E. Adman, and L. H. Jensen, *Proc. Natl. Acad. Sci. USA*. 1972, **69**, 3526.
10 C. W. Carter jun., in 'Iron-Sulphur Proteins,' ed. W. Lovenberg, Academic Press, New York, 1977, vol. 3, p. 158.
11 R. H. Holm and J. A. Ibers, in ref. 10, p. 205.
12 T. O'Sullivan and M. M. Millar, *J. Am. Chem. Soc.*, 1985, **107**, 4096; V. Papaefthymiou, M. M. Millar, and E. Munck, *Inorg. Chem.*, 1986, **25**, 3010.
13 B. A. Averill and W. H. Orme-Johnson, in 'Metal Ions in Biological Systems,' ed. H. Sigel, M. Dekker, New York 1978, vol. 7, p. 127.
14 D. G. Phillips and M. Poe in 'Iron-Sulphur Proteins,' ed. W. Lovenberg, Academic Press, New York, 1973, vol. 2, p. 225.
15 D. G. Nettesheim, T. E. Meyer, B. A. Feinberg, and J. D. Otvos, *J. Biol. Chem.*, 1983, **258**, 8235.
16 R. Krishnamoorthi, J. L. Markley, M. A. Cusanovich, C. T. Przysiecki and T. E. Meyer, *Biochemistry*, 1986, **25**, 60.
17 C. T. Przysiecki, T. E. Meyer, and M. A. Cusanovich, *Biochemistry*, 1985, **24**, 2542.
18 I. K. Adzamli, D. M. Davies, C. S. Stanley, and A. G. Sykes, *J. Am. Chem. Soc.*, 1981, **103**, 5543.
19 S. K. Chapman, C. V. Knox, and A. G. Sykes, *J. Chem. Soc., Dalton Trans.*, 1984, 2775.
20 G. Aprhamian and B. A. Feinberg, *Biochemistry*, 1981, **20**, 915.
21 I. A. Mizrahi, T. E. Meyer, and M. A. Cusanovich, *Biochemistry*, 1980, **19**, 4727.
22 J. R. Pladziewicz, A. J. Abrahamson, R. A. Davis, and M. D. Likar, *Inorg. Chem.*, 1987, **26**, 2058.
23 R. W. Callahan, G. M. Brown, and T. J. Meyer, *Inorg. Chem.*, 1975, **14**, 1443.
24 See, for example, L. Ebdon, S. Greenfield, and B. L. Sharp, *Chem. Br.*, 1986, **22**, 123.
25 See, for example, listing in A. G. Sykes, *Chem. Soc. Rev.*, 1985, **14**, 283.
26 See, for example, G. D. Armstrong, J. D. Sinclair-Day, and A. G. Sykes, *J. Phys. Chem.*, 1986, **90**, 3805.
27 R. J. Sundberg and G. Gupta, *Bioinorg. Chem.*, 1973, **3**, 39.
28 E. W. Miles, *Methods Enzymol.*, 1977, **47**, 431; N. Tudball, R. Bailey-Wood, and P. Thomas, *Biochem. J.*, 1972, **129**, 419.
29 D. G. Nocera, J. R. Winkler, K. M. Yocum, E. Bordignon, and H. B. Gray, *J. Am. Chem. Soc.*, 1984, **106**, 5145.
30 G. V. Buxton, *Adv. Inorg. Bioinorg. Mech.*, 1984, **3**, 131 and refs. therein.
31 E. M. Fielden, in 'The Study of Fast Processes and Transient Species by Electron Pulse Radiolysis,' ed. J. H. Baxendale and F. Busi, Reidel, Dordrecht, 1982, p. 58.
32 A. A. Frost and R. G. Pearson, in 'Kinetics and Mechanism,' 2nd edn., 1961, p. 49.
33 J. Butler, A. G. Sykes, G. V. Buxton, P. C. Harrington, and R. G. Wilkins, *Biochem. J.*, 1980, **189**, 641.
34 R. J. Crutchley, and W. R. Ellis, jun., H. B. Gray, in 'Frontiers in Bioinorganic Chemistry,' ed. A. V. Xavier, VCH, Weinheim, 1986, p. 679.
35 K. M. Yocum, J. B. Shelton, W. A. Schroeder, G. Worosila, S. S. Isied, E. Bordignon, and H. B. Gray, *Proc. Natl. Acad. Sci. USA*, 1982, **79**, 7052.
36 J. R. Winkler, K. M. Yocum, D. G. Nocera, E. Bordignon, and H. B. Gray, *J. Am. Chem. Soc.*, 1982, **104**, 5798; 1984, **106**, 5145.
37 S. S. Isied, C. Kuehn, and G. Worosila, *J. Am. Chem. Soc.*, 1984, **106**, 1722; R. Bechtold, M. B. Gardineer, A. Kazmi, B. van Hemelryck, and S. S. Isied, *J. Phys. Chem.*, 1986, **90**, 3800.
38 N. M. Kostic, R. Margalit, C.-M. Che, and H. B. Gray, *J. Am. Chem. Soc.*, 1983, **105**, 7765; R. Margalit, N. M. Kostic, C.-M. Che, D. F. Blair, H.-J. Chiang, I. Pecht, J. B. Shelton, J. R. Shelton, W. A. Schroeder, and H. B. Gray, *Proc. Natl. Acad. Sci. USA*, 1984, **81**, 6554.
39 R. Margalit, I. Pecht, and H. B. Gray, *J. Am. Chem. Soc.*, 1983, **105**, 301.
40 M. P. Jackman, A. G. Sykes, and G. A. Salmon, *J. Chem. Soc., Chem. Commun.*, 1987, 65; M. P. Jackman, J. M°Ginnis, R. Powls, G. A. Salmon, and A. G. Sykes, *J. Am. Chem. Soc.*, in the press.
41 J. P. Hoare, in 'Standard Potentials in Aqueous Solution,' eds. A. J. Bard, R. Parsons, and J. Jordan, Marcel Dekker, New York, 1985, p. 54.
42 R. A. Henderson and A. G. Sykes, *Inorg. Chem.*, 1980, **19**, 3103.
43 N. S. Hush, *Coord. Chem. Rev.*, 1985, **64**, 135.
44 R. A. Marcus and N. Sutin, *Biochim. Biophys. Acta*, 1985, **811**, 265.
45 S. L. Mayo and W. R. Ellis, jun., R. J. Crutchley, and H. B. Gray, *Science*, 1986, **233**, 948.

Received 30*th December* 1987; *Paper* 7/2267